Magnetic nanomanipulations inside living cells compared with passive tracking of nanoprobes to get consensus for intracellular mechanics

Damien Robert, Kelly Aubertin, Jean-Claude Bacri, and Claire Wilhelm*
Laboratoire Matière et Systèmes Complexes, CNRS UMR 7057, Université Paris 7, 75013 Paris, France
(Received 21 September 2011; published 9 January 2012)

During the last decade, the development of nanomaterials to penetrate inside living cells has been the focus of a large number of studies, with applications for the biomedical field. However, the further dynamics of these nanomaterials inside the cells is dictated by the intracellular environment and in particular its mechanical properties. The mechanical characteristics of the cell interior can be probed with either active or passive microrheological approaches. However, active intracellular microrheology is still in its infancy, owing to the difficulty of inserting probes that can be manipulated by external forces. Here we review recent active microrheology studies using magnetic nanoprobes inserted into endosomes or phagosomes as useful approaches for measuring frequency-dependent viscoelasticity, for mapping the viscoelastic landscape, as well as for identifying the contribution of individual cytoskeleton components and the influence of cell motility. The results of such direct measurements challenge the validity of more typical passive approaches in which the spontaneous displacement of embedded nanoprobes is measured. Here we discuss that one must distinguish probes suitable for use in conditions of thermal equilibrium, whose movements reflect the mechanical environment from probes that interact actively with the cytoplasm and cytoskeleton, in a state of nonequilibrium for which fluctuation-dissipation theorem no longer holds. However, when data on these probes' viscoelastic microenvironment is available, such passive probe movements can yield useful information on the forces responsible for intracellular activity.

DOI: 10.1103/PhysRevE.85.011905 PACS number(s): 87.17.Rt, 87.80.Fe, 83.10.Mj, 87.16.Uv

I. INTRODUCTION

Intracellular trafficking is a central issue in cell biology [1–3] and is directly influenced by the local viscoelasticity of the cytoplasm. Concommitantly, the recent development of nanomaterials has led us to design different types of nanoparticles to integrate living cells in order to import engineered functions [4–7]. This field of nanobiotechnology research grounds on the penetration of the nanoparticles inside the cells, and their subsequent intracellular becoming. The knowledge of the cell interior microenvironment therefore becomes a prerequisite for most of the nanobiotechnology applications.

Over the last two decades, microrheology has emerged as the leading technique for probing at the micro- and nanoscale mechanical properties in complex and heterogeneous media [8,9] such as living cells. Most microrheological techniques involve embedding micro- or nanoscale beads within the material of interest and studying their movement with one of two distinct approaches. In active microrheology, bead displacement is measured in response to an externally applied force, while passive microrheology examines spontaneous bead motion in response to local forces. The active approach can directly yield the frequency-dependent viscoelastic modulus $G^*(\omega)$. In contrast, because of the fluctuation dissipation theorem, passive microrheology requires the assumption that the system is in equilibrium in order to infer $G^*(\omega)$ from probe fluctuations.

So far, a large number of studies have characterized the cell's mechanical properties through the cell's outer membrane by using microbeads attached to membrane and associated cytoskeleton. Magnetic or optical tweezers are used to maneuver the beads and thus explore their physical microenvironment [10–12]. When probed at the cell surface, the complex shear modulus has then been found to exhibit frequency-dependent power-law behavior, $G^*(\omega) \sim G^*(\omega)^\alpha$, with α close to 0.2 [10,11,13], indicating predominantly elastic behavior. Fabry *et al.* [10] suggested that the physics of cell mechanics resembles that of soft glassy materials, in terms of structural complexity, metastability, and rearrangements.

Inside the cells, such direct measures of the microenvironment mechanical properties remain rare, due to the necessity to design probes that can be manipulated by external forces and that can also penetrate the cell interior. A promising alternative is to use the cell spontaneous endocytosis pathway to internalize probes that could be further manipulated. Due to the size cutoff of about 100 nm for the first endocytotic vesicular events, one must then call for nanotechnologies to design nanoscopic probes. Magnetic nanomaterials combine small enough size to penetrate the cell, and magnetic properties to allow manipulations at the nanoscale in the cell inside. In particular, the response of the so-called magnetic endosomes to a rotating magnetic field will infer the mechanical characteristics of the surrounding environment, in close relation to physical studies of the dynamics of chains of magnetic particles in a rotating magnetic field [14,15].

It must be noted that intracellular dynamics has been concomitantly extensively investigated by passively tracking spontaneous movements of injected [16,17] or endogenous intracellular nanoprobes [18,19], which, for systems in equilibrium, reveal the viscoelasticity of the probes' microenvironment. The mean square displacement (MSD) of such probes often shows a power-law diffusion in time, MSD $\sim t^\alpha$. However, both subdiffusive ($\alpha < 1$) and superdiffusive ($\alpha > 1$) motions have been reported for various probes inside living

*claire.wilhelm@univ-paris-diderot.fr

cells. Subdiffusive scaling was demonstrated for the motion of "inert" particles dispersed in the cytoplasm ($\alpha = 0.5$ for endogeneous granules [18,20,21], injected microspheres [16,22], and gold nanoparticles [23]) while intracellular organelles transported by molecular motors display superdiffusive scaling ($\alpha = 1.5$ for phagosomes) [24–28]. The fluctuation-dissipation theorem states that, for a system in equilibrium, the complex shear modulus can be inferred from the Fourier-transformed MSD, and that the deduced $G^*(\omega)$ follows a power-law increase with frequency, the exponent α being identical to that derived from the MSD time-dependent power-law trend. Inert probes used to determine the intracellular $G^*(\omega)$ show a power-law increase with frequency, and an exponent close to 0.5. However, any active (nonthermal) interaction of the probes with cytoplasmic or cytoskeleton components would prevent this derivation of $G^*(\omega)$, and the results must thus be interpreted with care.

Here we review intracellular magnetic manipulations using nanoprobes to investigate the cell interior mechanical properties, and to demonstrate that (i) the viscoelasticity landscape can be mapped at the microscale in the cell interior, and (ii) cell motility and the cytoskeleleton has a major influence on intracellular rheology. The results inferred by these magnetic nanorheology approaches challenge the largely used passive approaches. We then review representative passive intracellular studies with nanoprobes and compare their findings with the predictions of the fluctuation dissipation theorem. We discuss the validity of the passive approach and attempt to classify passive nanoprobes into two categories: those with no driving interactions with cell components, which can reliably be used to determine viscoelasticity; and those that interact actively with the cell, developing forces that can be extracted from their respective motions. Finally, we examine the few reported values for such active intracellular forces, in the pico-Newton range, deduced from rheological studies at the nanoscale.

II. MAGNETIC MANIPULATIONS OF INTRACELLULAR NANOPROBES

In active microrheology techniques, the probe is externally manipulated and the deformation of the medium is measured. What is needed therefore is a probe, situated at the very heart of the cell, that can be manipulated by applying external forces.

A few studies have used probes such as lipid granules that are already present in the cytoplasm and whose optical index allows them to be trapped and manipulated with "optical tweezers" [29,30]. The limiting factor in this approach is that only certain cell types contain such granules. Currently, the preferred approach consists of introducing magnetic particles, by endocytosis or phagocytosis, and then manipulating them with external magnetic fields.

Specialized cells such as macrophages and amoebae are capable of engulfing magnetic objects a few microns in size across in their interior, then located within membrane delimited vesicles, namely phagosomes, which can then be magnetically manipulated [27,31,32]. In contrast, with cells that are incapable of phagocytosing large objects (most cells including stem cells, immune cells, endothelial cells, muscle cells, etc.), the only available mechanism is endocytosis

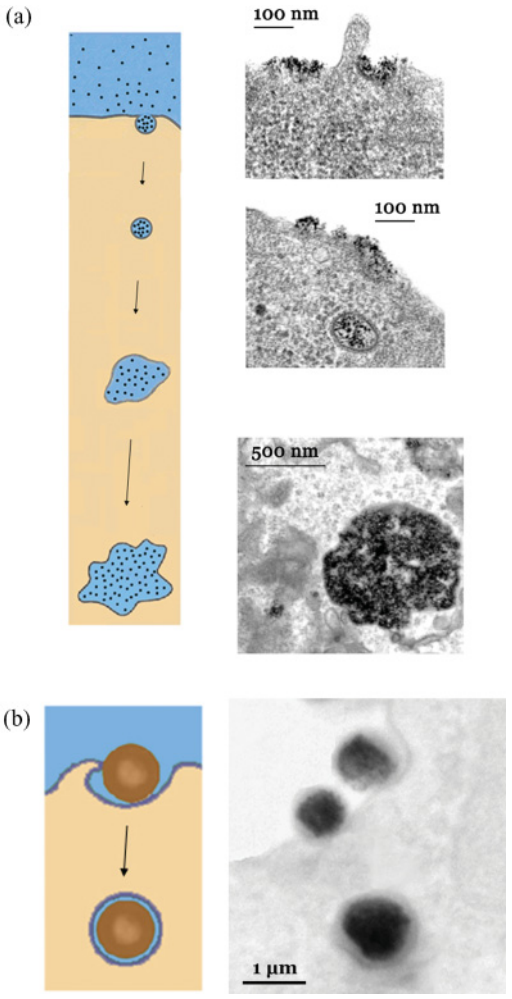

FIG. 1. (Color online) (a) Endocytosis of magnetic nanoparticules [diagram (left) and electron micrograph (right)]: the nanoparticules first attach to the plasma membrane. The membrane folds and detaches into 100-nm-diameter vesicles, encapsulating the magnetic nanoparticles. The vesicle then delivers its magnetic nanocontent to a succession of pre-existing membrane delimited compartments, endosomes. The nanoparticles end up densely confined into 600 nm in diameter final endosomes. (b) Phagocytosis of microbeads: the plasma membrane invaginates around the bead, detaches, and the subsequently formed magnetic phagosome migrates into the cytoplasm [diagram (left) and electron micrograph on amoeba (right)].

(Fig. 1), a process shared by all eukaryotic cells to internalize extracellular substances. During endocytosis, extracellular materials first attach to the cell membrane, the membrane then folds around the material, resulting in the formation of a small vesicle into which the material is incorporated. These primary endocytosis vesicles are only 100 to 200 nm in diameter, so that endocytosis is limited to objects less than a 100 nm across.

Nanomaterials are consequently the only candidates to be incorporated inside the cells through the endocytosis process. In particular, it has been demonstrated that iron oxide magnetic nanoparticles, in the range of 10 nm in diameter, follow the endocytotic pathway and easily penetrate the cell [33,34]. It is observed on electron microscopy images [Fig. 1(a)] that nanoparticles first interact with the plasma membrane, which then invaginates to form 100-nm-diameter endocytotic vesicles

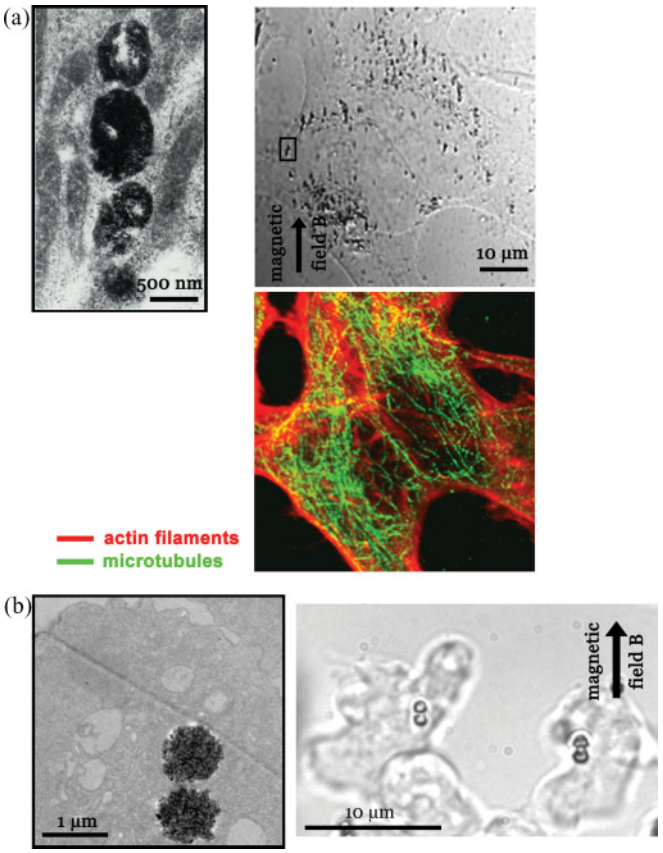

FIG. 2. (Color online) (a) Observations by electron microscopy (left) and video microscopy (center) of magnetic endosomes chaining. Chains are aligned in the direction of the applied magnetic field. Chains are immerged into the cytoskeleton, stained with fluorescent dyes [microtubules in green (light gray), delimited filaments, actin filaments in red (medium gray), at the cell periphery, more diffuse fluorescence] as shown on the right part of the figure. (b) Observations by electron microscopy (left) and video microscopy (right) of doublets of magnetic phagosomes aligned in the direction of an applied magnetic field B.

containing the nanoparticles, these first endocytotic vesicles being then delivered to endosomes. Finally, the nanoparticles become densely confined within endosomes with a mean diameter of 0.6 μm, becoming magnetic.

Similarly, in cells capable of phagocytosis (invagination of up to a few microns, to internalize larger objects), like macrophages or amoeba cells, magnetic microbeads could be localized inside the cytoplasm, into a phagosome compartment [Fig. 1(b)]. Magnetic endosomes or magnetic phagosomes then interact with one another when submitted to an external magnetic field and form doublets or small chains in the direction of the magnetic field (Fig. 2).

Initial studies of the mechanical properties of the cell interior examined internalized magnetic beads responses to an applied force or torque, fitting this temporal response to the simplest configuration of viscoelastic parameters. The models found to best represent intracellular mechanics were extensions of the Maxwell model (Kelvin-Maxwell or Voigt-Maxwell) [31,35–37]. The dynamics is dominated by elasticity during very short time periods, whereas over longer periods the medium behaves as a pure viscous liquid. Recently, however, studies using optically trapped intracellular granules or magnetic endosomes and phagosomes invalidated this approach by demonstrating that the microrheological behavior of the cell interior is accurately described by power laws [27,29,30,38]. This power-law behavior indicates that intracellular dynamics is not tied to a particular relaxation time. A continuum of relaxation times is inconsistent with the discrete number of time constants predicted by simple viscoelastic models. By contrast, an infinity of Maxwell simple mechanical units (dashpot and spring in series) associated in parallel, with relaxation times τ_i distributed according to a power-law $P(\tau_i) \sim {\tau_i}^{1-\alpha}$, is described by a complex frequency f -dependent shear modulus $G^*(f) \sim (if)^\alpha$.

Figure 3 documents this power-law behavior in two cell models, a highly motile amoeba or a poorly motile tumor cell. In the tumor cells, the magnetic probes are magnetic endosomes filled with iron oxide nanoparticles, while in the amoeba, which are phagocyting cells, 1 μm magnetic beads engulfed into phagosomes are used. Under the effect of an in-plane oscillating magnetic field, the chains of magnetic endosomes or phagosomes can be oscillated at the field frequency f [Fig. 3]. The loss of angular amplitude, and the temporal phase-lag relative to the external field, directly yield the complex viscoelastic modulus at frequency f, $G^*(f) = G'(f) + iG''(f)$, where G' and G'' relate to the elastic and the viscous response of the intracellular material, respectively. For any probe oscillating between 0.2 and 20 Hz, at any intracellular location, the resulting G' and G'', behaves as $G'(f)$, $G''(f) \sim f^\alpha$, with the same exponent α, that is the complex modulus follows itself power-law $G^*(f) = G_o(if)^\alpha$. Power-law behavior is therefore a robust characteristic of the cell interior at the microscale. It is found in cells with very different functions, from strongly adherent poorly motile tumor cells to continuously motile amoeba cells. In the former cells the cytoskeleton (especially actin filaments) serves as a mechanical support, while in the latter its main role is to develop propulsive forces. For the tumor cells, the average stiffness was found close to $G'(1\text{ Hz}) = 15$ Pa, with an average exponent $\alpha = 0.4$ [38]. By contrast, an average stiffness $G'(1\text{ Hz}) = 2$ Pa was measured for the amoeba cell, was much lower than that of the tumor cells, reflecting a softer medium, with an average exponent $\alpha = 0.54$ found higher [27].

The exponent α places itself as the signature of the liquid ($\alpha = 1$) versus solid ($\alpha = 0$) like behavior. For tumor cells, the value of the exponent ($\alpha = 0.4$) shows that the behavior is more elastic than viscous. In contrast, the cytoplasm of motile amoeba cells is more fluid, with $\alpha = 0.54$, in agreement with differences in motility.

One advantage of internalized magnetic nanoprobes is that they are contained in endosomes or phagosomes vesicles dispersed throughout the cytoplasm, and can thus be used to obtain an accurate map of intracellular viscoelasticity. Figure 4 shows variations in the viscoelasticity of single cells probed with magnetic endosomes [in poorly motile tumor cells, Fig. 4(a)] or with magnetic phagosomes [in highly motile amoebae, Fig. 4(b)]. The measured G' (1 Hz) values are color coded according to their amplitude, between 0.1 and 40 Pa. Both cells exhibited marked subcellular mechanical heterogeneity.

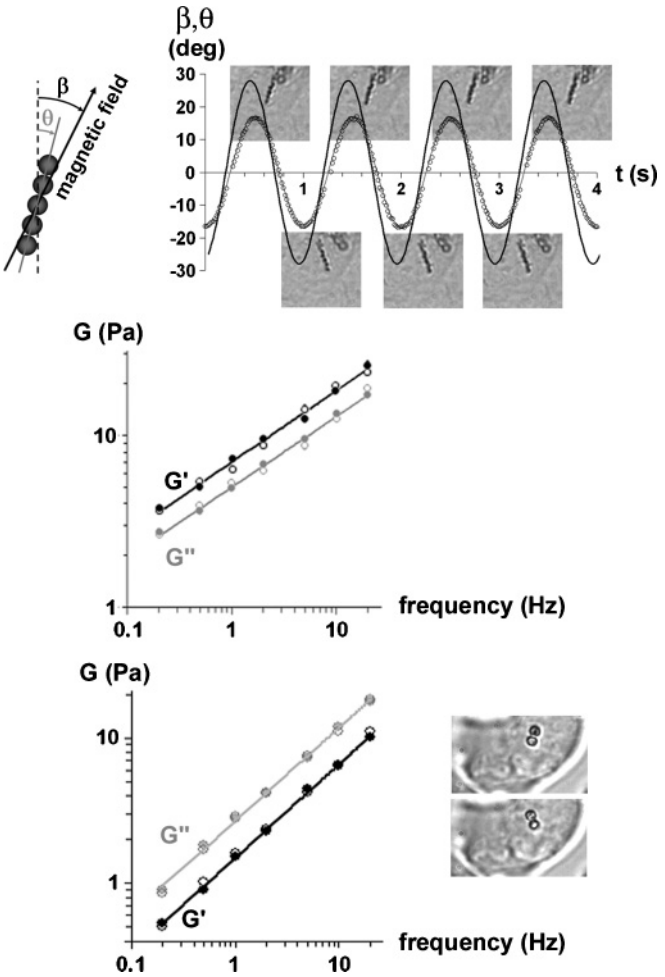

FIG. 3. Top: Typical angular curve of a chain of endosomes, oscillating at 1 Hz (open symbols), in response to the [−28 deg, 28 deg] oscillation of the magnetic field (plain curve). Middle and bottom: The viscoelastic moduli are calculated from the loss in amplitude $\theta o/\beta o$ and the phase lag ϕ of the chains of endosomes in tumor cells (middle) or phagosomes in amoeba (bottom; example of oscillation of a chain of phagosomes at 0.2 Hz in the inset). By making the chains oscillate at different frequencies (between 0.2 and 2 Hz), one can derive for each probe chain the frequency dependence of the viscoelastic modules G' and G'', that obey a power law. After a series of measurement at increasing frequencies (plain symbols), the frequency was systematically decreased (open symbols), ensuring that the viscoelastic moduli inferred were not modified, that is that the measure is not damageable for the cell microenvironment.

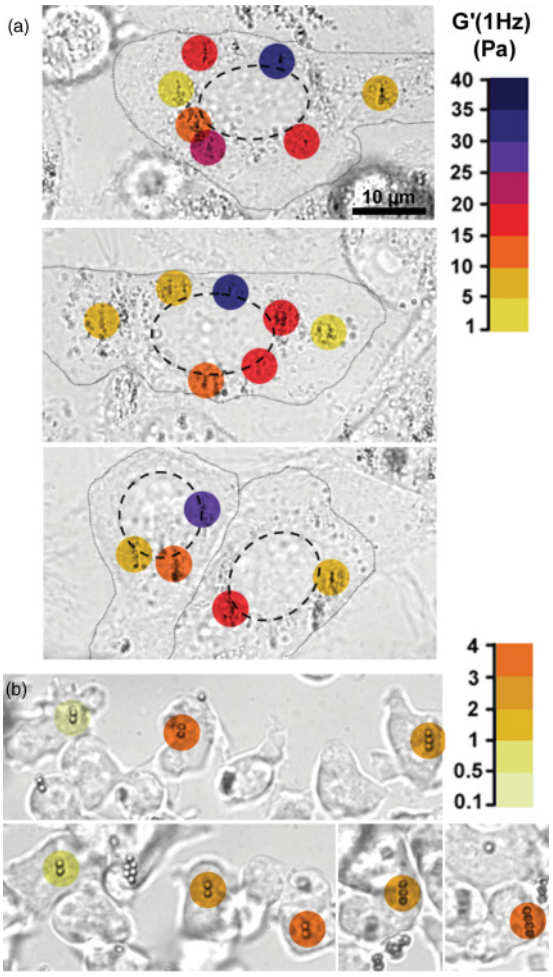

FIG. 4. (Color online) Intracellular viscoelasticity mapping. For tumor cells (a), the membrane is represented by small dashes and the nucleus by large dashes. Inside tumor cells (a) or amoeba cells (b), one can distinguish several chains of endosomes or phagosomes, respectively, which serve to probe their microenvironment. The viscoelasticity thus measured [here $G'(1\ \text{Hz})$ is indicated] is color coded and superimposed on the images.

Such local determination of viscoelastic intracellular properties has been rarely performed inside a single cell. Using active microrheology, only Yanai *et al.* [29] demonstrated regional differences between the leading and trailing regions of locomoting neutrophils. However, these specific intracellular regions are devoted to cell locomotion, with a major role of actin filaments at the leading edge into which the probes are englued. Moreover, in the case of this study, granules were manipulated with optical tweezers, making it possible to only perform the measure on one single probe at one single time. Using magnetic endosomes or phagosomes rheology, regional difference at the scale of the cytoplasm itself is demonstrated, including no specific regions, and the measure is performed simultaneously in a single cell, for probes at different location. The only other intracellular mechanical studies to give such pictures of cell heterogeneities for single cell use passive microrheology: different probes can then be easily tracked simultaneously, and the viscoelasticity inferred at their different positions [39,40]. However, passive microrheology needs the assumption that the system is at thermal equilibrium, as discussed in the next paragraph. These previous passive microrheological studies of the cell inside have demonstrated a high degree of subcellular mechanical heterogeneity. Such a heterogeneity is an expected signature for the internal microenvironments of the cells, which are a complex, heterogeneous combination of flexible cytoskeletal filaments and viscous liquid containing membrane-delimited organelles. This high degree of heterogeneity of the cell cytoplasm is confirmed thanks to the local mapping of the viscoelastic moduli inferred with no assumption through magnetic nanoprobes active microrheology.

TABLE I. Active intracellular microrheology studies: the probes used, the exponent value, and the stiffness at 1 Hz G' (1 Hz) are listed. Ranges of values obtained by active measurement with a membrane-bound probe are indicated. For intracellular measurements, a star indicates new analyses of the temporal response to a constraint, implying a power law for the viscoelastic module (rather than a mechanical model with a finite number of elements used in the original publications).

	Cells	Probes	Exponent α	G'(1Hz) (Pa)	Ref.
Measure at the membrane	Epithelial, Muscle, Tumor, Myoblasts	Microbeads, Microplates	0.18–0.22	300–3000	[10,11]
Active microrheology inside the cell	Macrophages	Phagosomes	0.3–0.4⋆	100	[31]
	Amoeba	Phagosomes	0.6⋆	40	[35]
	Amoeba	Phagosomes	0.5⋆	40	[51]
	Tumor cells	Endosomes	0.5⋆	3	[52]
	Granulocytes	Phagosomes	0.6–0.7⋆	9	[37]
	Neutrophils	Granules	0.5	1.5	[29]
	Epithelial cells	Granules	0.3	10	[30]
	Amoeba	Phagosomes	0.5–0.6	1–10	[27]
	Tumor cells	Endosomes	0.4	10–40	[38]

To assess the influence of cytoskeleton components on the intracellular power-law rheology, microtubules and actin filaments were selectively disrupted in tumor cells [38]. Figure 5 shows the viscoelasticity mapping after one of the two cytoskeleton components had been disrupted. It is to note that

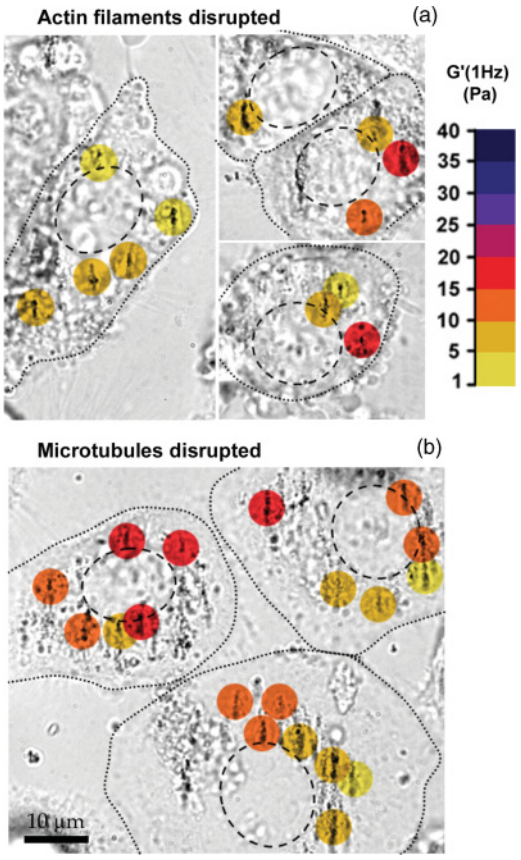

FIG. 5. (Color online) Viscoelasticity inside tumor cells with disrupted actin filaments or disrupted microtubules. The value of the viscoelastic module G' (1 Hz) is color coded and superimposed on the chains of intracellular endosomes in tumor cells in which either the actin filaments (a) or microtubules (b) have been destroyed.

the power law is conserved for each probe induced to oscillate at different frequencies in the absence of actin filaments or microtubules. However the average viscoelasticity is found lower than that of the control conditions, with G' (1 Hz) around 10 Pa when microtubules are disrupted and close to 7 Pa when actin filaments are disrupted, reflecting a softer medium and less heterogeneous. Moreover, the exponents were found somewhat higher, with a mean value of $\alpha = 0.48$ in the absence of microtubules and $\alpha = 0.56$ in the absence of actin filaments, demonstrating that microtubules and actin filaments contribute to the elasticity of the cytoplasm.

Table I summarizes values obtained in other active intracellular microrheology studies. These values comprise the exponent corresponding to that of the power law of $G(f)$. Using the first active measurements made in the temporal domain and fitted with mechanical models to certain relaxation times, a power-law behavior can also be extracted from the data. The recalculated exponent is also shown in Table I, with a star designating the new data analysis.

All studies yield values in the range 10–100 Pa for the viscoelastic module at 1 Hz and an exponent in the range 0.3–0.7. It is interesting to note the differences between these values and those obtained using membrane-bound probes, the range of which (also shown in Table I) is 300–3000 Pa for the viscoelastic module at 1 Hz, with an exponent of about 0.2. It clearly states that the intracellular medium is less rigid than the membrane, and also more fluid (exponent values).

III. CAN PASSIVE AND ACTIVE MICRORHEOLOGY WITH NANOPROBES INSIDE THE CELLS GET TOGETHER TO A CONSENSUS?

In passive microrheology the motion of an internally embedded probe is simply tracked, and its relation with the local physical microenvironment is inferred [41]. Many types of passive probe have been tested, differing in size (from nanometers [23] to microns [25,42]), material (gold [23], polymer microspheres [16]), and the internalization process (microinjected [17,40,43], endocytosed [44,45], or

endogeneous [18,19,40,42]). The time-lag dependence mean square displacement of each probe $\langle r^2(t)\rangle$ (MSD), is computed from its track. $\langle r^2(t)\rangle$ is often accurately fitted by a power-law $\langle r^2(t)\rangle \sim t^\alpha$ in which the exponent α reflects the type of movement observed. Subdiffusion is indicated by α values between 0 and 1, and usually corresponds to the signature of a probe embedded in a viscoelastic network. Superdiffusion is revealed by α values above 1, which show that the probe is subject to active motion.

Passive microrheology assumes that, for a system in equilibrium, $\langle r^2(t)\rangle$ reflects the viscoelastic nature of the microenvironment. Indeed, the fluctuation dissipation theorem (FDT) states that the complex shear modulus can be directly inferred from the Laplace-transformed $\langle r^2(t)\rangle$, $\langle r^2(i\omega)\rangle$: $G^*(\omega) = kBT/[i\pi\omega a\langle r^2(i\omega)\rangle]$. The exponent of $G^*(\omega)$ is then the same as for $\langle r^2(t)\rangle$. Through the FDT it is possible to anticipate from active measurements of G^* the mean square displacement of an intracellular probe in conditions of thermal equilibrium. Using the active measurements described in the previous paragraph, in conditions of thermal equilibrium, the $\langle r^2(t)\rangle$ of the probes should vary with t^α, at α values between 0.3 and 0.7. At equilibrium, the $\langle r^2(t)\rangle$ of the probes is inversely proportional to their diameter a. This is why, when comparing values of their spatial excursions, it is necessary to calculate the product $a\langle r^2(t)\rangle$. Figure 6 shows $a\langle r^2(t)\rangle$ values obtained in representative studies. The shaded range shows the expected range of $a\langle r^2(t)\rangle$ values in thermal equilibrium. This range was obtained by reversing the FDT from G^* values obtained by active microrheology, assuming an average exponent of 0.5. It appears that endogenous granules and microinjected probes are situated in this range of spatial excursion [16,18]. Moreover, the exponent values thus obtained are close to 0.5. These probes have been widely used to derive the viscoelastic module, which is then found to exhibit power-law behavior with an exponent of about 0.5, in keeping with direct measurements. Another noteworthy approach to put the system at the in equilibrium situation consisted of making passive measurements in the absence of ATP (inhibited by sodium azide) [13,46]. Passive measurements on 4.5 μm beads phagocytosed by epithelial cells then leads to a power-law behavior with exponent 0.26, and with rigidity in the appropriate range.

The case of probes internalized by endocytosis and phagocytosis is quite different. Thus, endocytosed 100-nm beads have a superdiffusive $\langle r^2(t)\rangle$ over several orders the range expected at equilibrium, and an exponent of 1.25 [47]. Also shown are the displacements $\langle r^2(t)\rangle$ of magnetic endosome and phagosome probes used as well in active microrheology. For all these internalized probes, equilibrium is clearly disrupted at times exceeding 0.1 s. It should however be kept in mind that, at far shorter times, endocytosed probes can also reflect the mechanical environment: in this case there is a transition between a subdiffusive regime at short time scales and a superdiffusive regime at longer time scales, as observed in [44] for 1 μm phagosomes, with a subdiffusive regime appearing at times shorter than 0.1 s. Another noteworthy approach to measuring probe fluctuations used gold nanobeads injected into the cell, which distinguishes between the two behaviors [23]. The MSD then follows a power law with an exponent of 0.5, but with values far above those assumed to exist at

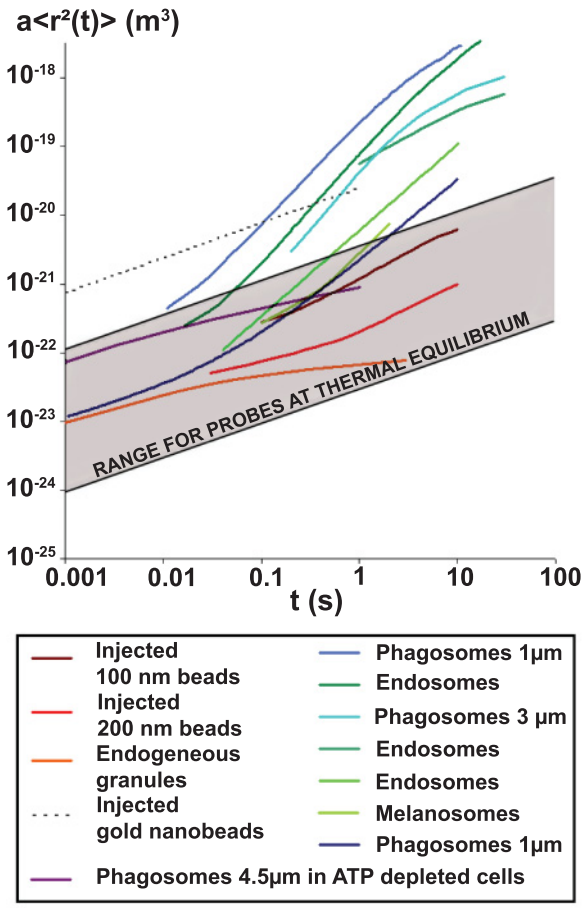

FIG. 6. (Color) Mean square intracellular displacements of various probes: endogenous granules (in orange [18]), injected 200 nm beads (in red [16]) or 100 nm beads (in brown [17]), endosomes in tumor cells (in dark green [38]; in bright green [47]; in blue-green [53]), melanosomes (in mid-green [49]), phagosomes in : fibroblasts (in bright blue [25] and in dark blue [44]), Dictyostelium cells (in blue [27]), and ATP depleted epithelial cells (in purple [13]), and injected gold nanobeads (in dotted line [23]). The gray range corresponds to the expected window for intracellular probes movement at the in equilibrium situation and is provided by the active microrheology measurements, which lead to a viscoelastic modulus G' at 1 Hz in between 1 Pa (lower limit in the figure) and 100 Pa (upper limit) thermal equilibrium, with power-law behavior with exponent close to 0.5.

equilibrium. However, these are the only true "nanometric" probes (diameter below 10 nm), and it is likely that the probed medium corresponds to intracellular microfields that are less rigid than larger microscale domains, and that were never probed with active microrheology using probes less than 10 nm in diameter.

The very large variations noted in these passive microrheology studies illustrate the difficulty of interpreting these data.

However, several studies yielded values in the range obtained by active measurement, namely 10–100 Pa for the viscoelastic module at 1 Hz and an exponent of about 0.5, demonstrating once more that the intracellular medium is less rigid than the membrane, and also more fluid (exponent values).

IV. SPONTANEOUS DISPLACEMENT OF INTRACELLULAR PROBES: A CLUE TO ACTIVE INTRACELLULAR FORCES?

In the case of vesicular transport of probes within a cell, with violation of equilibrium, it becomes challenging to extract from the probes tracks information on the forces that drive the probes activity. These active forces are fundamental because they permit intracellular trafficking, incessant nanovesicles transport between the different compartments of the intracellular space. This intense trafficking relies on a protein microtubule network capable of serving all parts of the cell. The transport is driven by the two large families of microtubule-associated molecular motors, dyneins and kinesins. It is the forces generated by these molecular motors that are responsible for the shift from equilibrium observed with internalized probes, which are an integral part of the intracellular vesicular system.

The most popular approaches to obtaining information on the motor forces presence inside a cell consisted of dissecting the probes spontaneous motions mostly via their calculated mean square displacement (MSD) $\langle r^2(t)\rangle$. The first type of study showed the role of cytoskeleton constituents, and especially microtubules, in the emergence of an exponent above 1 for the MSD, reflecting the activity of intracellular motors [24,25]. The same type of approach was used to demonstrate active transport to the nucleus [48]. However, several assumptions are necessary to draw direct inferences on these forces from the exponent. Thus, other authors used a viscoelastic model, corresponding to a spectrum of power-law forces [49]. The idea was to measure the local slope of $\langle r^2(t)\rangle$, to adjust the viscoelastic model to the exponent thus obtained, and thereby to deduce the active force spectrum. This approach is particularly attractive. However, the exponent obtained for the thermal force spectrum was 1, corresponding to purely viscous behavior and conflicting with direct measurements of viscoelasticity. Another recent approach was to define temporal windows and to calculate the MSD in these windows only [40,50]. It was then possible to discriminate from the exponent and the direction the active and passive transport components. Then, forces of about 0.2 pN were obtained for phagosomes in *Dictyostelium* [50], much less than the force developed by molecular motors (about 5 pN).

Within this framework of attempts to gain insights into intracellular forces through the spontaneous displacements of immerged probes, emerges a conspicuous need to first access the viscoelastic landscape of the probes. Initial measures taking into account the properties of the probes surrounding medium used magnetic phagosomes submitted to an external magnetic field gradient. The working hypothesis was that the medium surrounding the phagosome was a simple viscous liquid, as the force was applied continuously and the situation corresponded to a dissipative regime. Movement towards the force provided information on the viscosity, while perpendicular movement shed light on fluctuations of active forces. The forces thus measured were between 50 and 200 pN [35,51]. The limiting factor of such studies stands in the necessary hypothesis that the magnetic force applied throughout the measure does not affect the activities of the motors on the phagosome, and consequently its directed motion.

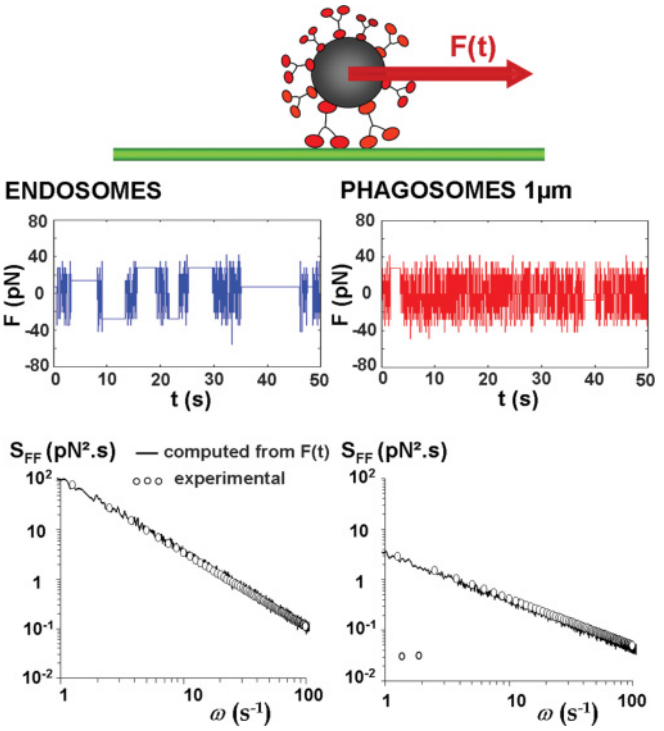

FIG. 7. (Color online) Endosomes and phagosomes are equipped with molecular motors that allow them to move along microtubules. It is thus possible, by using a combination of active and passive microrheology, to experimentally determine the spectrum (S_{FF}) of the active force F responsible for the movement of these vesicles (circles). These spectra can then be simulated very simply (lines) by constructing F as a function of time, as time-distributed instantaneous forces. These instantaneous forces can reach several tens of pN, with an average of about 20 pN for endosomes and phagosomes.

Finally, one promising approach is to use the combination of independent measurements of fluctuation (passive microrheology) and dissipation (active microrheology) on the same probes in order to experimentally derive the power spectrum of the active intracellular forces acting on these probes [19,27,38]. Indeed, a generalized Langevin equation is sufficient to show that this force spectrum can be expressed as the product of the viscoelastic module and the Fourier transform of $\langle r^2(t)\rangle$. Figure 7 shows a typical force spectrum obtained for an endosome or a phagosome. It is then possible to model these experimentally obtained spectra and thus to derive the motor force $F(t)$ acting on each of these vesicles. This force is intermittent and variable, with application times that are temporally distributed according to a power law. The amplitude of these applied forces yields the instantaneous force that motors are capable of exerting on endosome or phagosome; this force can reach about 100 pN, with an average of about 20 pN for endosomes [38] with a mean diameter of 0.6 μm and for phagosomes 1 μm in diameter [27]. It varies linearly with the radius of the phagosome, from about 5 pN for phagosomes 0.3 μm in diameter to 50 pN for phagosomes 2.8 μm in diameter. It should be remembered that, in the case of active vesicle transport, molecular motors interact with microtubules—linear protein filaments—to permit intracellular trafficking. This explains the linear growth in force as the diameter of the

spherical vesicle increases: of all the molecular motors coating the spherical vesicle, only those located along a diameter which when projected is tangential to a given microtubule, will participate in the movement and the motor density available for force generation depends thus in principle on the radius of the vesicles concerned. It must finally be emphasized that by comparison thermal forces generated on micron sized probes entrapped inside the intracellular viscoelastic medium (with exponent 0.5 and G' at 1 Hz in between 1 and 100 Pa, as described by active microrheology experiments) are in the 0.01–0.5 pN range, that is approximately two orders of magnitude smaller that the active forces responsible for the vesicular trafficking. In this context, no assumptions of thermal equilibrium can be validated.

V. CONCLUSIONS

To measure the local viscoelasticity inside the cell, one promising approach is to use the spontaneous endocytosis of magnetic nanoparticles to get intracellular nanoprobes that can be piloted by external magnetic fields. It is then demonstrated that power-law frequency dependent behavior is a robust signature of intracellular rheology, whatever intracellular location, with an average exponent of 0.4 for poorly motile tumor cells and 0.6 for highly motile amoeba cells. Motile cells display a more liquid-like cytoplasm than strongly adherent cells. For these latter cells, the cytoskeleton is the main actor to provide the increase of the elastic contribution to the microrheological behavior, its disruption leading to a more liquid medium.

The few existing active intracellular microrheological studies meet together to state that the intracellular medium is accurately described by power law with exponent close to 0.5 and is less rigid and more liquid than the membrane and associated cytoskeleton. In contrast, behaviors based on spontaneous intracellular probe fluctuations (passive microrheology) tend to diverge. It is then necessary to distinguish probes that are not subject to active interactions with the cytoplasm and whose spontaneous movements reflect the rheological behavior from probes such as endosomes and phagosomes that interact actively with the cytoskeleton. With these latter probes it becomes possible to use their observed movements to derive information on the forces that drive their activity. One particularly promising approach is to use combined measurements of fluctuation and dissipation in order to experimentally derive the spectrum of active intracellular forces.

[1] N. Hirokawa, Y. Noda, Y. Tanaka, and S. Niwa, Nat. Rev. Mol. Cell Biol. **10**, 682 (2009).
[2] L. N. Patel, J. L. Zaro, and W. C. Shen, Pharm. Res. **24**, 1977 (2007).
[3] R. D. Vale, Cell **112**, 467 (2003).
[4] A. P. Alivisatos, W. Gu, and C. Larabell, Annu. Rev. Biomed. Eng. **7**, 55 (2005).
[5] N. L. Rosi and C. A. Mirkin, Chem. Rev. **105**, 1547 (2005).
[6] A. Solanki, J. D. Kim, and K. B. Lee, Nanomedicine (London) **3**, 567 (2008).
[7] K. M. Krishnan, IEEE Trans. Magn. **46**, 2523 (2010).
[8] A. R. Bausch and K. Kroy, Nat. Phys. **2**, 231 (2006).
[9] B. D. Hoffman and J. C. Crocker, Annu. Rev. Biomed. Eng. **11**, 259 (2009).
[10] B. Fabry, G. N. Maksym, J. P. Butler, M. Glogauer, D. Navajas, and J. J. Fredberg, Phys. Rev. Lett. **87**, 148102 (2001).
[11] M. Balland, N. Desprat, D. Icard, S. Fereol, A. Asnacios, J. Browaeys, S. Henon, and F. Gallet, Phys. Rev. E Stat. Nonlin. Soft Matter. Phys. **74**, 021911 (2006).
[12] X. Trepat, L. Deng, S. S. An, D. Navajas, D. J. Tschumperlin, W. T. Gerthoffer, J. P. Butler, and J. J. Fredberg, Nature (London) **447**, 592 (2007).
[13] B. D. Hoffman, G. Massiera, K. M. Van Citters, and J. C. Crocker, Proc. Natl. Acad. Sci. USA **103**, 10259 (2006).
[14] T. Ukai, H. Morimoto, and T. Maekawa, Phys. Rev. E. Stat. Nonlin. Soft Matter. Phys. **83**, 061406 (2011).
[15] M. Belovs and A. Cebers, Phys. Rev. E. Stat. Nonlin. Soft Matter. Phys. **79**, 051503 (2009).
[16] Y. Tseng, T. P. Kole, and D. Wirtz, Biophys. J. **83**, 3162 (2002).
[17] C. M. Hale, S. X. Sun, and D. Wirtz, PLoS One **4**, e7054 (2009).
[18] S. Yamada, D. Wirtz, and S. C. Kuo, Biophys. J. **78**, 1736 (2000).
[19] A. W. C. Lau, B. D. Hoffman, A. Davies, J. C. Crocker, and T. C. Lubensky, Phys. Rev. Lett. **91**, 198101 (2003).
[20] B. Yap and R. D. Kamm, J. Appl. Physiol. **98**, 1930 (2005).
[21] C. Selhuber-Unkel, P. Yde, K. Berg-Sorensen, and L. B. Oddershede, Phys. Biol. **6**, 025015 (2009).
[22] Y. Tseng, J. S. Lee, T. P. Kole, I. Jiang, and D. Wirtz, J. Cell Sci. **117**, 2159 (2004).
[23] G. Guigas, C. Kalla, and M. Weiss, Biophys. J. **93**, 316 (2007).
[24] H. Salman, Y. Gil, R. Granek, and M. Elbaum, Chem. Phys. **284**, 389 (2002).
[25] A. Caspi, R. Granek, and M. Elbaum, Phys. Rev. Lett. **85**, 5655 (2000).
[26] D. Weihs, T. G. Mason, and M. A. Teitell, Biophys. J. **91**, 4296 (2006).
[27] C. Wilhelm, Phys. Rev. Lett. **101**, 028101 (2008).
[28] M. Brunstein, L. Bruno, M. Desposito, and V. Levi, Biophys. J. **97**, 1548 (2009).
[29] M. Yanai, J. P. Butler, T. Suzuki, H. Sasaki, and H. Higuchi, Am. J. Physiol. Cell Physiol. **287**, C603 (2004).
[30] M. T. Wei, A. Zaorski, H. C. Yalcin, J. Wang, S. N. Ghadiali, A. Chiou, and H. D. Ou-Yang, Opt. Express **16**, 8594 (2008).
[31] A. R. Bausch, W. Moller, and E. Sackmann, Biophys. J. **76**, 573 (1999).
[32] W. Moller, I. Nemoto, T. Matsuzaki, T. Hofer, and J. Heyder, Biophys. J. **79**, 720 (2000).
[33] C. Wilhelm, F. Gazeau, J. Roger, J. N. Pons, and J. C. Bacri, Langmuir **18**, 8148 (2002).
[34] O. Lunov, V. Zablotskii, T. Syrovets, C. Rocker, K. Tron, G. U. Nienhaus, and T. Simmet, Biomaterials **32**, 547 (2011).
[35] W. Feneberg, M. Westphal, and E. Sackmann, Eur. Biophys. J. **30**, 284 (2001).
[36] C. Wilhelm, F. Gazeau, and J. C. Bacri, Phys. Rev. E Stat. Nonlin. Soft. Matter. Phys. **67**, 06190801 (2003).

[37] A. H. de Vries, B. E. Krenn, R. van Driel, and J. S. Kanger, Biophys. J. **88**, 2137 (2005).
[38] D. Robert, T. H. Nguyen, F. Gallet, and C. Wilhelm, PLoS One **5**, e10046 (2010).
[39] S. R. Heidemann and D. Wirtz, Trends Cell Biol. **14**, 160 (2004).
[40] M. H. Duits, Y. Li, S. A. Vanapalli, and F. Mugele, Phys. Rev. E Stat. Nonlin. Soft Matter. Phys. **79**, 051910 (2009).
[41] T. G. Mason and D. A. Weitz, Phys. Rev. Lett. **74**, 1250 (1995).
[42] S. S. Rogers, T. A. Waigh, and J. R. Lu, Biophys. J. **94**, 3313 (2008).
[43] T. P. Kole, Y. Tseng, I. Jiang, J. L. Katz, and D. Wirtz, Mol. Biol. Cell **16**, 328 (2005).
[44] M. Jonas, H. Huang, R. D. Kamm, and P. T. So, Biophys. J. **95**, 895 (2008).
[45] C. Picard and A. Donald, Eur. Phys. J. E Soft Matter **30**, 127 (2009).
[46] K. M. Van Citters, B. D. Hoffman, G. Massiera, and J. C. Crocker, Biophys. J. **91**, 3946 (2006).
[47] N. Gal and D. Weihs, Phys. Rev. E Stat. Nonlin. Soft Matter. Phys. **81**, 020903 (2010).
[48] J. Suh, D. Wirtz, and J. Hanes, Proc. Natl. Acad. Sci. USA **100**, 3878 (2003).
[49] L. Bruno, V. Levi, M. Brunstein, and M. A. Desposito, Phys. Rev. E Stat. Nonlin. Soft Matter. Phys. **80**, 011912 (2009).
[50] D. Arcizet, B. Meier, E. Sackmann, J. O. Radler, and D. Heinrich, Phys. Rev. Lett. **101**, 248103 (2008).
[51] D. Heinrich and E. Sackmann, Acta Biomater. **2**, 619 (2006).
[52] C. Wilhelm, J. Browaeys, A. Ponton, and J. C. Bacri, Phys. Rev. E Stat. Nonlin. Soft Matter. Phys. **67**, 011504 (2003).
[53] R. P. Kulkarni, M. Bak-Maier, and S. E. Fraser, Proc. Natl. Acad. Sci. USA **104**, 1207 (2007).